17th World Conference on Earthquake Engineering, 17WCEE
Sendai, Japan - September 13th to 18th 2020

An Attempt to Evaluate the Characteristics of a Building in Terms of Predominant Periods, Natural periods and Apparent Torsions

S. Inoue[(1)], T. Ota[(2)] and H. Watanabe[(3)]

[(1)] Graduate School of Engineering Course Student, Kanto Gakuin University, m19J3006@kanto-gakuin.ac.jp
[(2)] Researcher, Institute of Science and Technology, Kanto Gakuin University, m16J3003@kgu.jp
[(3)] Associate Professor, Kanto Gakuin University, hwatanab@kanto-gakuin.ac.jp

Abstract

This is an inquiry into the properties and characteristics of a building in terms of predominant periods, natural periods and apparent torsions by using the data recorded in the 46 earthquakes of seismic intensity 3 or greater out of 213 ones of seismic intensity 1 or greater observed in the building. Predominant periods and natural periods were calculated by the Fourier spectra which were outputted from the FFT method of accelerations obtained by strong motion seismometers. Among the peak periods in the Fourier spectrum ratios, the peak period with the largest Fourier spectral ratio value was defined as the predominant period, and the longest peak period was defined as the first natural period. And the approximation line was calculated by the acceleration orbits drawn by the data from the strong motion seismometers. The apparent torsion in this paper was the value which was the difference the gradient of the approximation line in the upper floor with it in the bottom floor, divided by the height from the upper floor to the bottom. The calculated results show that the natural periods tended to increase with the increase of I_{JMA}. The highest angle of apparent torsion was recorded when the longitudinal axis dimension of the building matched the azimuth of the epicenter. It was from the data between 3F and 1F, not between RF and 7F. The eigenvalue analysis was calculated by using an abbreviated equation and was compared with the measured natural periods at the same time. The eigenvalue analysis showed that the natural period was longer than the natural period calculated by using an abbreviated equation. Also, it is clear that no serious damage occurred to the building, so far. Further consideration will be given to our previous paper[1] in this paper, referring to the latest data.

Keywords: seismic observation, existing building, seismic retrofit, first natural period, damage criteria

Introduction

One of the ways to grasp the vibration characteristic of a structure is to install seismometers in it and to observe the response of the building towards earthquakes. It makes use of structure health monitoring such as the damage detection and the evaluation the soundness of the building. Seismic observation has been continued on a re-reinforced medium-rise steel-reinforced concrete building named Kawamoto-ind., which is located in Naka-ward, Yokohama, Japan since 20 February, 2015. The six strong motion seismometers have recorded the response acceleration time history in three directions; longitudinal(X), transverse(Y) and vertical(Z). The purpose of this research is not only to clarify the health and safety of the building which has experienced various levels of earthquakes through these records, but also to confirm the validity of continuous use of monitoring systems in seismic observation. Also, it aims to contribute to an adequate introduction of judgement criteria that will help quickly determine the damage extent of re-reinforced steel reinforced concrete buildings in case it experience a massive earthquake in the future. Ota and others (2016, 2017 and 2018) made a report on the dynamic characteristics of the building which could be inferred from the records for two months from February, 2018. Kajiwara and others (2018) reported the characteristic of the target building through dominant periods, first natural periods and apparent torsions. In this report, we made use of only the information obtained by the seismometers installed in the building, which was not equipped with the software devised by Kusunoki (2005). They recorded the seismic intensity of 1 or greater 213 times during the research period. In this paper, we will evaluate the properties and characteristics of the

building in terms of predominant periods, natural periods and apparent torsions from these 213 records. And then we suggested some preparatory criteria for judging damage of this building, showing data from the latest seismic observation.

Target building and Observation System

Fig.1 (a) shows the present state of the target building, which was completed in 1973, and Table 1 shows its specifications. In 2014, 38 steel framed braces were set in the 1st to 7th floors, and 21 columns were bound with steel plates in the 1st to 3rd floors as seismic retrofitting for the existing building. The first horizontal natural period on the re-reinforced building is calculated by using the following two methods.

a) by using an abbreviated equation (1), with H=30.5m.

$$T_1=0.02H \quad (1)$$

b) by using eigenvalue analysis concerning the natural period in the longitudinal direction, T_{iL} and that in the transverse direction, T_{iT}, which are obtained based on the lateral stiffness and weights of each story, taking into consideration the secondary walls in the allowable stress design. The building is assumed to be an 8-lumped mass with the column on the 1st floor fixed at the bottom end in eigenvalue calculation of b). Table 2 shows the natural periods T_{iL} and T_{iT} in each direction of each mode order i based on b).

Table 1 Specification of the building

Location	Naka-ward, Yokohama, Japan
Main uses	Offices
Number of stories	Two stories underground, eight stories above ground, one-story penthouse
Height	30.5m
Structure	Steel encased reinforced concrete
Complete	1973
Retrofit	2014

Table 2 Natural periods of each mode based on b)

direction		1st	2nd	3rd	4th	5th	6th	7th	8th
X	T_{iL}[s]	0.72	0.27	0.17	0.12	0.10	0.09	0.08	0.07
Y	T_{iT}[s]	0.82	0.32	0.21	0.15	0.12	0.10	0.09	0.08

Table 3 Specifications of the seismometers

sampling	noise	acceleration range
[Hz]	[cm/s/s]	[cm/s/s]
100	0.1	±2450

Fig.1 (b) shows the layout of the seismometers. The six strong motion seismometers, which have been set at 100Hz in three directions; longitudinal(X), transverse(Y) and vertical(Z), have been installed on B2F, 1F, 3F, 5F, 7F and RF. Another seismometer was installed on the 7th floor during 23 February, 2015, and 15 April, 2016 to measure the eccentricity of the building. Table 3 shows the specifications of seismometers. Table 4

shows details of the earthquake of seismic intensity 3 or greater measured on the building, and Fig.2 shows the acceleration wave forms observed in an earthquake just for an example.

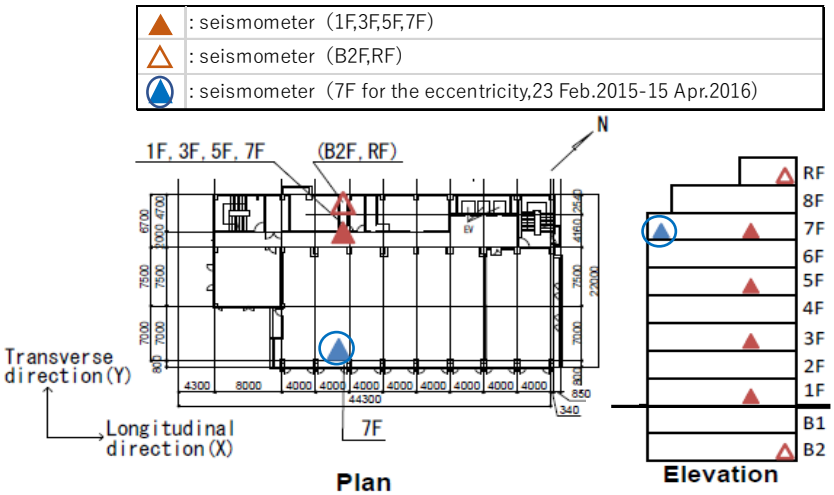

(a) east view of Kawamoto Ind. Building (b) layout of measuring equipment

Fig.1 Outline of the building and layout of the seismometers

Analysis method

Predominant periods and natural periods were calculated by the Fourier spectra which were outputted from the FFT method of the acceleration. These spectra smoothed with Parzen window at a band width of 0.2Hz in the FFT method. Transfer functions were calculated by using Fourier spectrum ratios based on the first floor. The microtremor was not included in the analysis that the natural period might not be evaluated as a short period. Therefore, the only secondary waves were targeted with the number of data being a power of 2. The secondary wave part was selected visually, and the maximum response value was included in the analysis target time, based on the response acceleration time history of the second underground level. The periods were considered on the top floor as a representative in this research. Some peak periods could be seen in the Fourier spectrum ratios. The peak periods in the target building were not considered when they were shorter than T_{8L}=0.07s and T_{8T}=0.08s from Table 2. Among the peak periods, the peak period with the largest Fourier spectral ratio value was defined as the predominant period, and the longest peak period was defined as the first natural period.

Fig.3 shows Fourier spectrum ratios on RF/1F, 7F/1F, 5F/1F, 3F/1F and B2F/1F. In this Figure, in the X (longitudinal) direction, the dominant period is 0.72s, the primary natural period is also 0.72s, in the Y (transverse) direction, the dominant period is 0.45s, the primary natural period is 0.73s, the 2nd or 3rd order mode is prominent, as a result.

Table 5 shows the ratio of outstanding modes for the data with seismic intensity 3 or greater. The first predominant mode in X (longitudinal) direction accounts for 72.3% and following 3rd mode appeared 19.1%. The 3rd mode account for 74.5% in Y (transverse) direction, and it can be inferred that the higher order mode is dominant. Especially the first mode never appears in the Y (transverse / short side) direction.

Table 5 The appearance ratio of predominant mode (the number of times) [%]

direction \ mode	1st	2nd	3rd	4th
X(longitudinal)	72.3	6.4	19.1	2.1
Y(transverse)	0.0	21.3	74.5	4.3

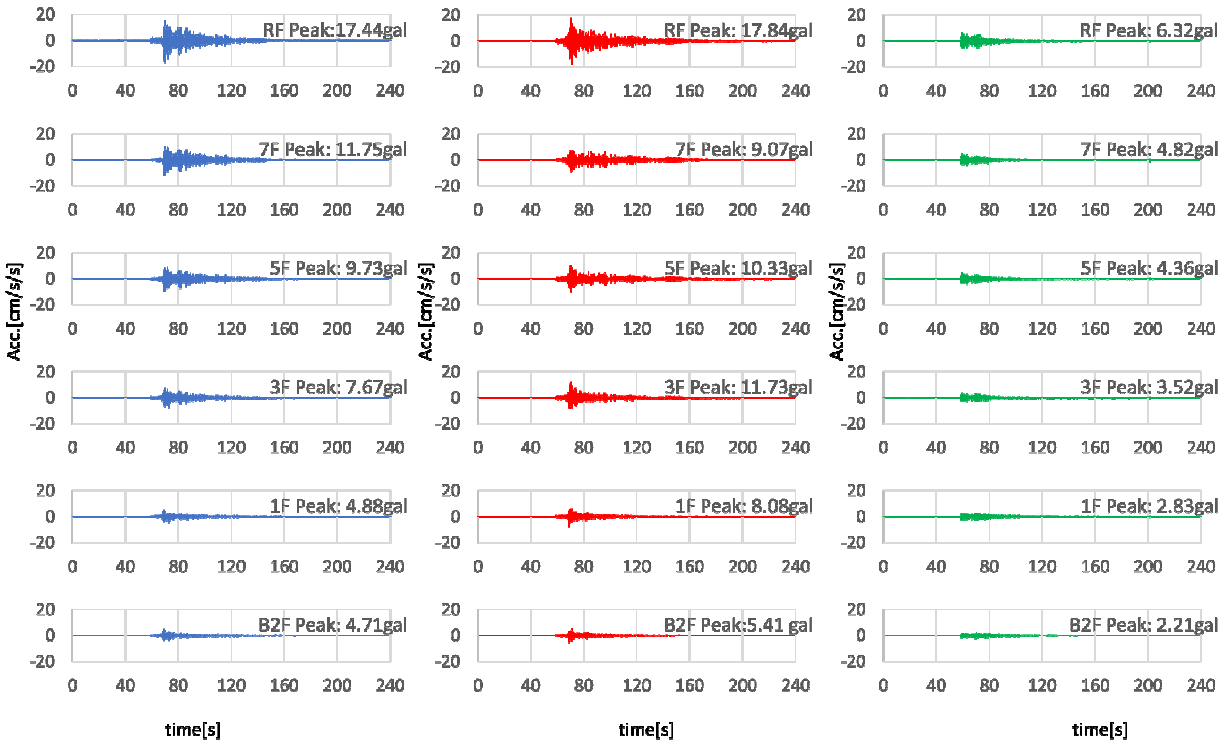

(a)Transverse (b)Longitudinal (c)Vertical

Fig.2 Observed acceleration waveforms (25 May, 2019 EQ)

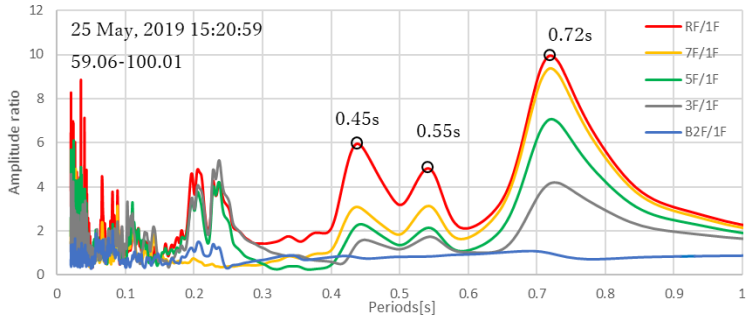

(a) X (longitudinal) direction

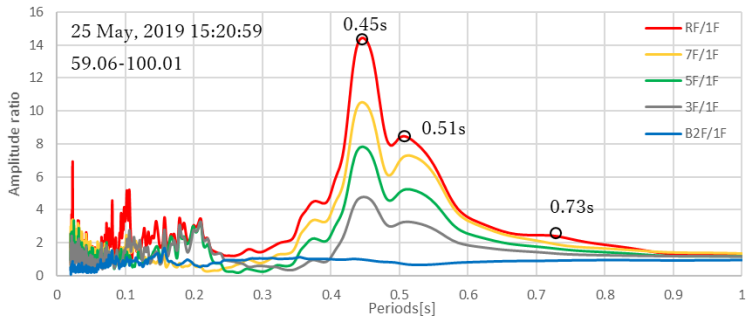

(b) Y (transverse) direction

Fig.3 Fourier spectrum ratios (25 May, 2019 EQ)

Table 4 Details of the earthquake of seismic intensity 3 or greater measured on the building

No.	Date	I_{JMA}* (JMA Scale)	from Japan Meteorological Agency H.P.[6]				
			epicenter (JMA)	the North latitude[°] (JMA)	the East latitude[°] (JMA)	focal depth[km] (JMA)	Magnitude Mj** (JMA)
1	23 Feb., 2015	2.53	NW Chiba Pref.	35.56	140.14	68	4.5
12	13 May, 2015	3.20	Off Miyagi Pref.	38.86	142.15	46	6.8
14	25 May, 2015	4.26	N Saitama Pref.	36.05	139.64	56	5.5
17	30 May, 2015	4.89	W off Ogawasara Is.	27.86	140.68	6.82	8.1
37	12 Sep., 2015	3.60	Tokyo Bay	35.55	139.83	57	5.2
41	24 Oct., 2015	2.71	NW Chiba Pref.	35.80	140.08	66	3.7
51	5 Feb., 2016	3.70	E Kanagawa Pref.	35.63	139.54	26	4.6
53	7 Feb., 2016	2.71	S Ibaraki Pref.	36.05	139.90	43	4.6
62	16 May, 2016	4.29	S Ibaraki Pref.	36.03	139.89	42	5.5
68	17 Jul., 2016	3.56	S Ibaraki Pref.	36.04	139.93	42	5.0
69	19 Jul., 2016	3.30	NE Chiba Pref.	35.42	140.35	33	5.2
70	20 Jul., 2016	3.00	S Ibaraki Pref.	36.02	139.95	42	5.0
72	27 Jul., 2016	2.78	N Ibaraki Pref.	36.45	140.61	57	5.4
80	7 Sep., 2016	2.65	S Ibaraki Pref.	36.17	140.04	50	4.9
83	13 Sep.,2016	3.52	S Saitama Pref.	35.94	139.81	77	4.9
90	26 Oct., 2016	2.79	NW Chiba Pref.	35.81	140.11	64	4.1
92	17 Nov., 2016	2.62	NW Chiba Pref.	35.65	140.16	66	4.2
94	22 Nov., 2016	3.88	Off Fukushima Pref.	37.35	141.60	25	7.4
97	24 Nov., 2016	2.67	Off Fukushima Pref.	37.17	141.35	24	6.2
101	28 Dec., 2016	3.00	N Ibaraki Pref.	36.72	140.57	11	6.3
106	19 Feb., 2017	2.65	E Off Chiba Pref.	35.73	140.66	52	5.4
107	28 Feb., 2017	2.68	Off Fukushima Pref.	37.51	141.37	52	5.7
117	13 Jun., 2017	2.56	NW Chiba Pref.	35.79	140.10	63	3.8
121	2 Aug., 2017	2.77	N Ibaraki Pref.	36.80	140.54	9	5.5
123	3 Aug., 2017	2.86	S Ibaraki Pref.	36.08	139.89	46	4.6
124	10 Aug., 2017	3.58	NW Chiba Pref.	35.80	140.09	64	5.0
132	6 Oct., 2017	2.80	Off Fukushima Pref.	37.09	141.16	53	5.9
139	27 Dec., 2017	2.56	Tokyo Bay	35.57	140.08	69	4.5
141	6 Jan., 2018	3.92	Tokyo Bay	35.64	140.02	71	4.7
146	26 Feb., 2018	3.08	Off Fukushima Pref.	37.54	141.76	40	5.8
154	4 May, 2018	2.71	NW Chiba Pref.	35.65	140.18	69	4.2
155	4 May, 2018	2.61	NW Chiba Pref.	35.65	140.17	69	4.1
157	15 May, 2018	2.58	E Yamanashi Pref/Fuji Five Lakes	35.49	139.02	27	4.3
158	17 May, 2018	2.68	NE Chiba Pref.	35.72	140.73	52	5.3
169	7 Jul., 2018	4.08	E Off Chiba Pref.	35.16	140.60	66	6.0
172	14 Aug., 2018	2.58	E Off Chiba Pref.	35.20	140.55	59	4.7
183	27 Nov., 2018	3.31	S Ibaraki Pref.	36.07	139.86	44	5.0
218	18 Jan., 2019	3.02	N Ibaraki Pref.	35.92	140.43	54	5.3
222	25 May, 2019	3.15	NE Chiba Pref.	35.35	140.29	38	5.1
223	1 Jun., 2019	2.57	NE Chiba Pref.	35.37	140.29	35	4.7
228	24 Jun., 2019	3.89	E Off Izu Peninsula	35.07	139.10	8	4.1
232	25 Jul., 2019	2.58	E Off Chiba Pref.	35.15	140.57	58	5.1
233	28 Jul., 2019	2.72	SE Off Mie Pref.	33.16	137.40	393	6.6
235	4 Aug., 2019	3.60	Off Fukushima Pref.	37.71	141.63	45	6.4
241	12 Oct., 2019	3.13	SE Off Chiba Pref.	34.67	140.65	75	5.4
245	22 Nov., 2019	2.72	S Ibaraki Pref.	36.07	139.89	45	4.5

I_{JMA}*:Maximum measured seismic intensity on the building

Mj**: Magnitude

The apparent torsion angles were considered from the acceleration records on each measurement floor. The apparent torsion which is per unit height to the bottom floor was obtained by dividing the rotation angle of the principle axis of the upper floor plane with the principle axis of the lower floor plane by the distance between the seismometers. In Fig.4, the trajectories of the acceleration called as *acceleration orbits* are indicated by the black solid line in the X (longitudinal) direction and the Y (transverse) direction. And the approximation line was calculated by the acceleration orbits drawn by the data from the strong motion seismometers. The approximate straight line by using the least squares method are indicated by red numerical lines. The approximate lines in red thus were assumed to be the *principle axes* here. It can be seen that the principle axes are shown mainly along the X (longitudinal) direction.

Analytical results

Fig.5 shows the temporal change of the predominant periods and the first natural periods from 20 February, 2015 to 22 November, 2019. The maximum of the predominant period was obtained in an earthquake on 30 May, 2015 in the X (longitudinal) direction, in an earthquake on 25 May, 2015 in the Y (transverse) direction, respectively. These values were 0.79s in X (longitudinal) direction, and 0.55s in Y (transverse) direction. The predominant periods were 0.42s to 0.79s in the X (longitudinal) direction and 0.37s to 0.55s in the Y (transverse) direction. Comparing the minimum and the maximum values, they correspond to a change in horizontal stiffness of 28% in the X (longitudinal) direction and 47% in the Y (transverse) direction. The maximum of the first natural period was 0.79s obtained in an earthquake on 30 May, 2015 in the X (longitudinal) direction. In the Y (transverse) direction, it was 0.89s recorded in an earthquake on 5 February, 2016.The earthquake on 30 May, 2015, which gave the maximum value of the first natural period in the X (longitudinal) direction, was the earthquake with a hypocenter at an azimuth angle of 173°. The earthquake on 5 February, 2016, which gave the maximum value of the first natural period in the Y (transverse) direction, was the earthquake with a hypocenter at an azimuth angle of 337°. The first natural periods were 0.60s to 0.79s in the X (longitudinal) direction and 0.69s to 0.89s in the Y (transverse) direction. Comparing the minimum and the maximum values, they correspond to a change in horizontal stiffness of 74% in the X (longitudinal) direction and 61% in the Y (transverse) direction. The first natural period using by an abbreviated equation was T_1=0.61s, and these periods using by eigenvalue analysis, the secondary walls in the allowable stress design taken into consideration, were T_{1L}=0.72s, T_{1T}=0.82s from Table 2. It means that the eigenvalue analysis shows that the natural period was longer than the natural period calculated by using an abbreviated equation. And the horizontal stiffness of this building can be relatively lower because the measured natural periods could be longer than the calculated natural periods such as T_1, T_{1L} and T_{1T}. However, this building has not been damaged with serious injury since the tendency of the first natural periods has not been increasing after 30 May, 2015 in X (longitudinal) direction and 5 February, 2016 in Y (transverse) direction which were the maximum records of the first natural periods.

Fig.6 shows the relationships between the first natural period and the azimuth angle, the peak maximum response acceleration, and the measured seismic intensity. The peak maximum response accelerations were made dimensionless by dividing by the gravitational acceleration. The same figure also shows the following two values; the average value of the ratios of the approximate straight lines in the X (longitudinal) and Y (transverse) directions obtained by the least squares method to the values obtained from the approximate straight lines for the measured values of the first natural period (m) and coefficient of variation ($C.V$). The relationship between the first natural period and the measured seismic intensity gives the smallest coefficient of variation, and the first natural period in each direction tends to increase with the increase of the measured seismic intensity.

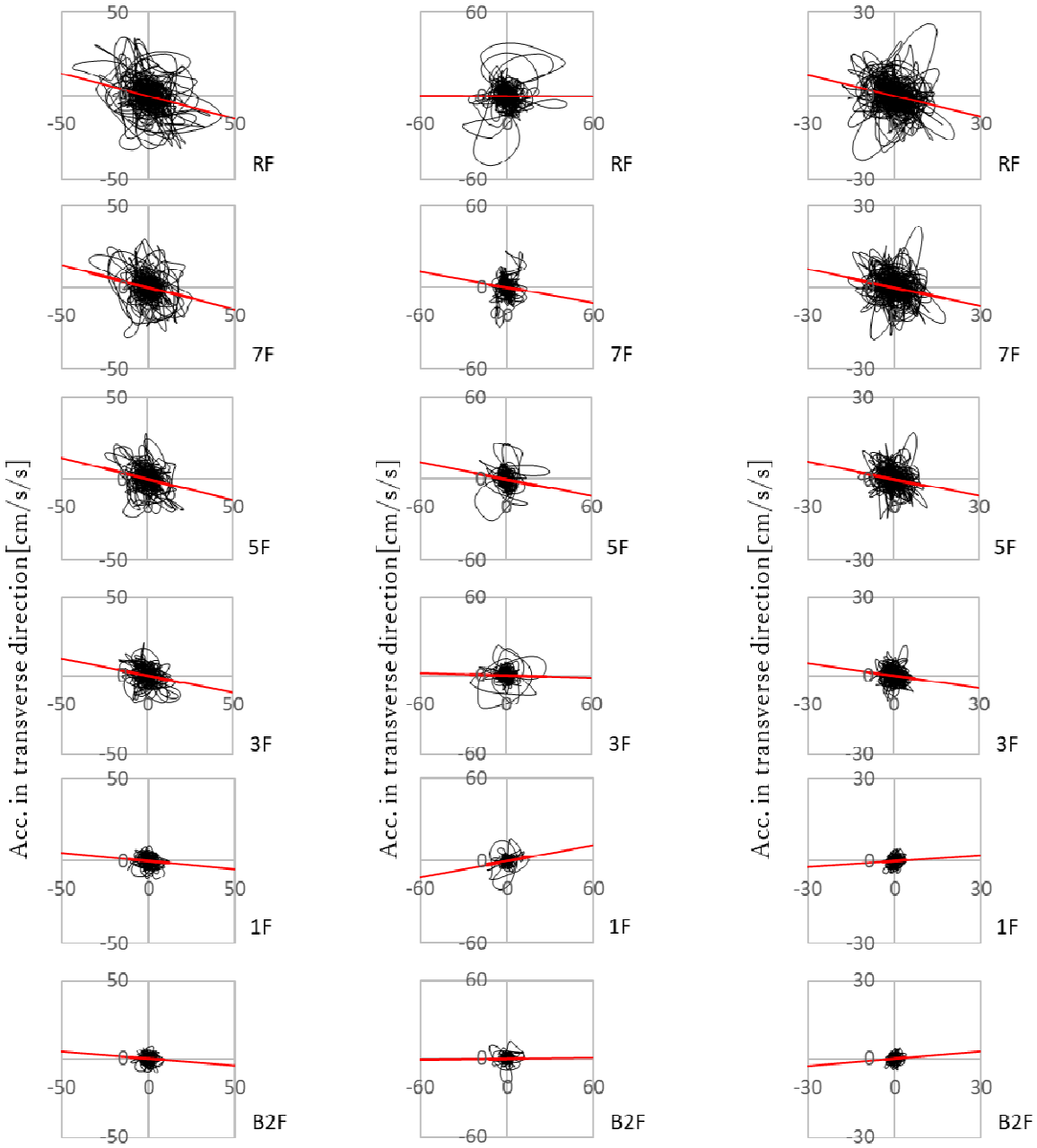

(a) 7 Jul., 2018 EQ (b)24 Jun., 2019 EQ (c)4 Aug., 2019 EQ

Fig.4 Acceleration orbits and assumption of a principal axes

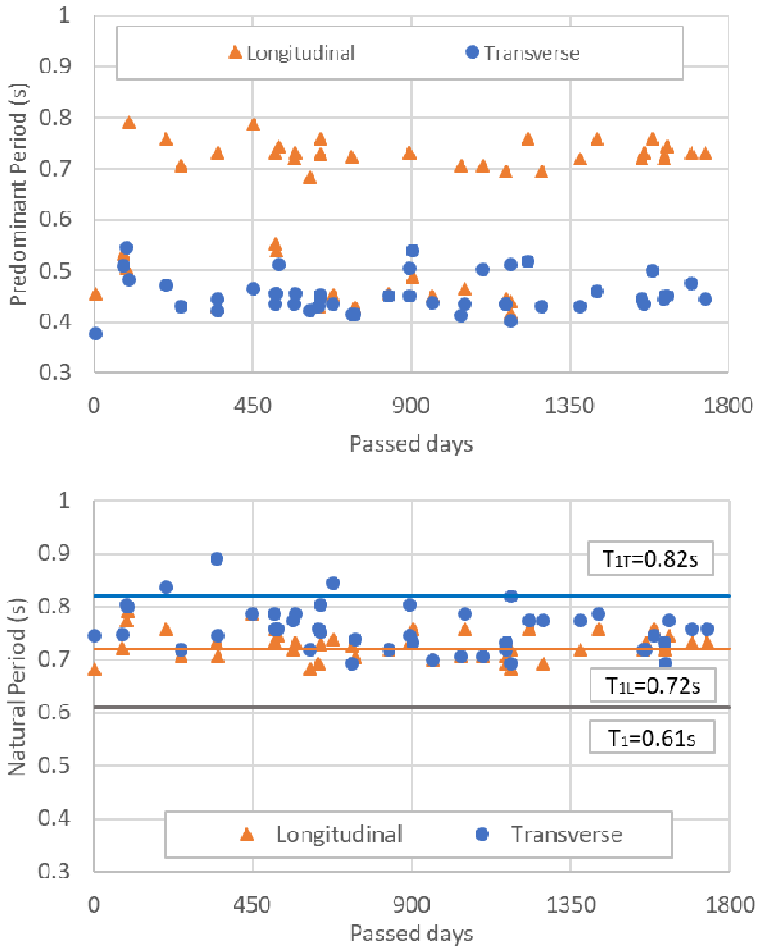

Fig.5 Change over time in the Predominant periods and the first natural periods
(20 Feb., 2015-22 Nov., 2019)

Fig.7 indicates the change over time in the angle θ of apparent torsion per unit of length between each measurement floor. The apparent torsion angle is not relatively large between RF to 7F on the top, but it is relatively large between 3F and 1F. The maximum value of the apparent torsion angle θ in the target building was obtained between 3F and 1F in an earthquake on 10 August, 2017. It can be confirmed from the subsequent earthquake records that no significant increase in the apparent torsional angle occurred. The examination of the apparent torsion angle will be continued in the future.

Fig.8 indicates the relations between the angle of apparent torsion per unit length and the azimuth, and the maximum response acceleration at each floor, and the measured seismic intensity. Here, the maximum response acceleration of each floor is indicated as the square root of sum of squares of vectors in two horizontal directions. No correlation between measured seismic intensity and maximum response acceleration and apparent torsion angle was found compared with the primary natural periods. On the other hand, there is a tendency that the apparent torsional angle between 3F and 1F increases in an earthquake with an hypocentral direction at an azimuth angle of 45° which is nearly equal to the angle of the X (longitudinal) direction in the building. The earthquake in 10 August, 2017 which was the highest record of the apparent torsion was I_{JMA} 3.58 with an hypocentral direction at an azimuth angle of 46°. Since there are also azimuthal angles of earthquakes that the building has not experienced, it will be necessary to grasp its behaviors against earthquakes in various azimuths in the future.

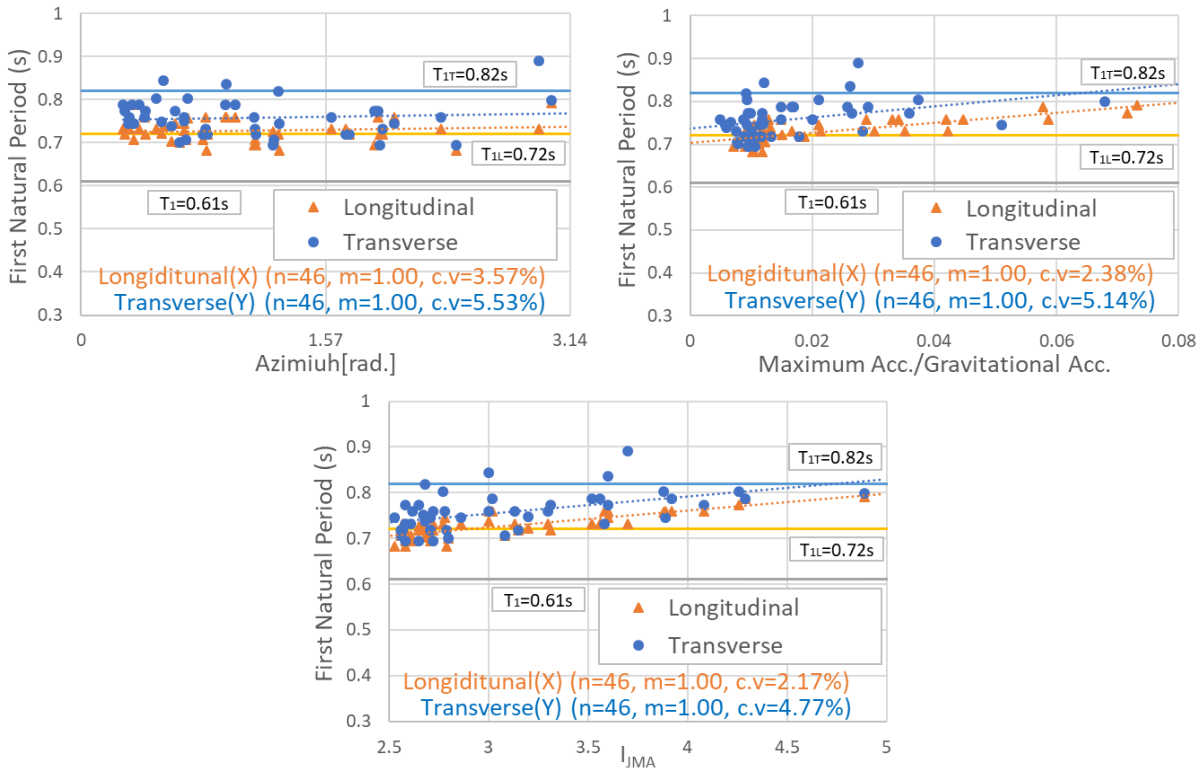

Fig.6 Relations among the first natural periods,
and the Azimuth, and the Maximum Acc./Gravitational Acc., and I_{JMA}
(20 Feb., 2015-22 Nov., 2019)

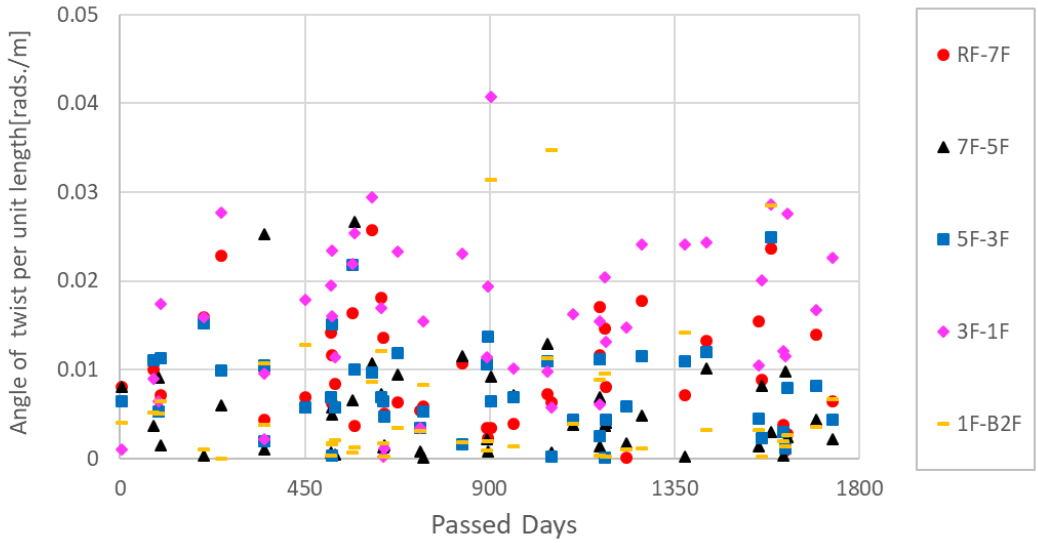

Fig.7 Change over time in the angle of apparent torsion per unit of length
(20 Feb., 2015-22 Nov., 2019)

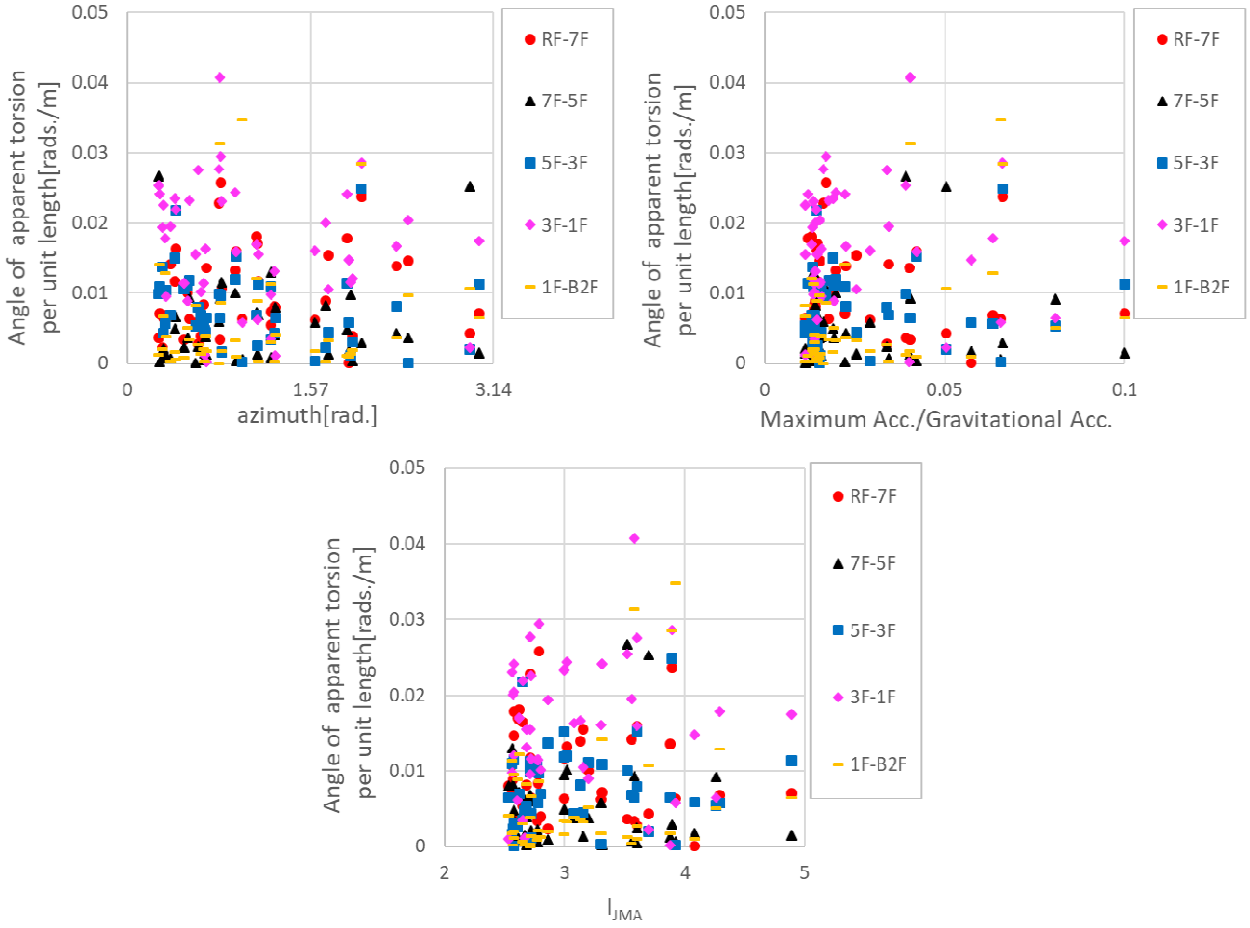

Fig.8 Relations among the angle of apparent torsion per unit of length, and the Azimuth, and the Maximum Acc./Gravitational Acc., and I_{JMA}

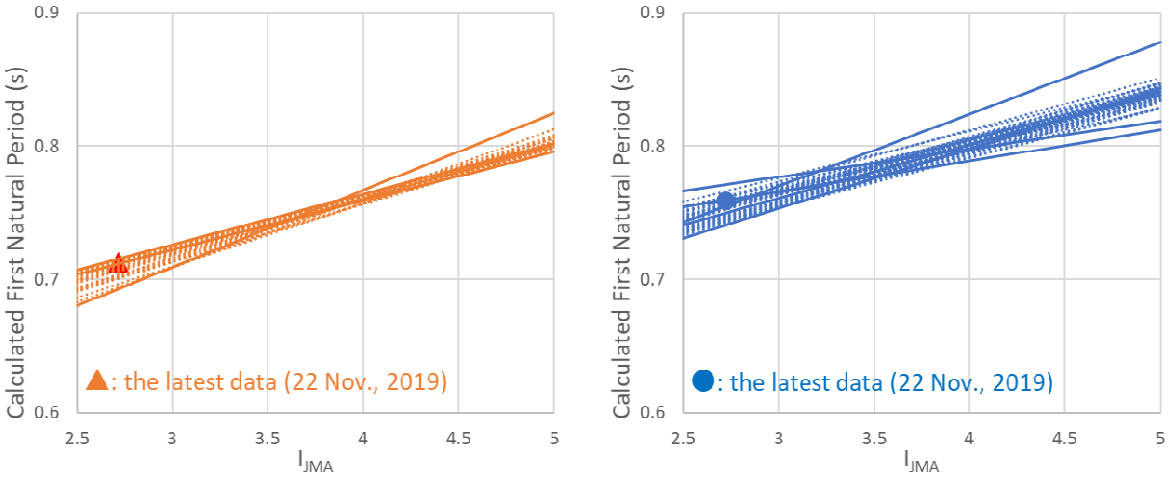

(a) X (longitudinal) direction (b) Y (transverse) direction

Fig.9 Relations between the calculated first natural periods and I_{JMA}

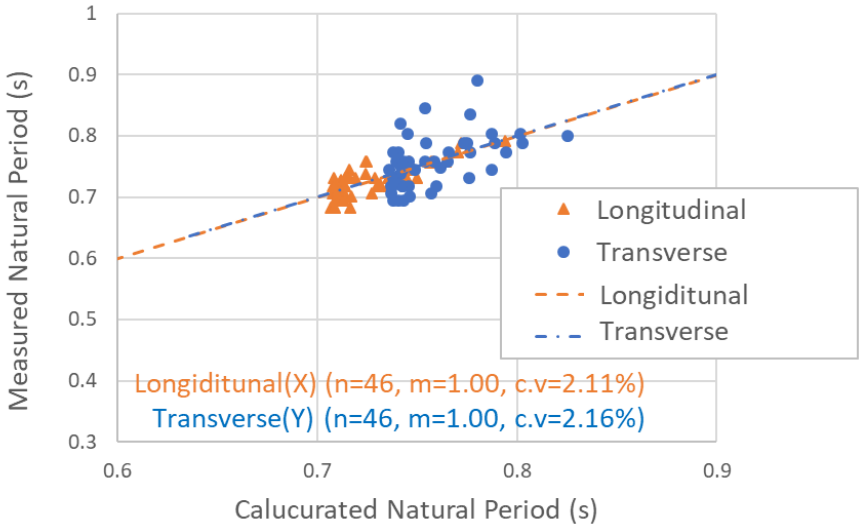

Fig.10 The calculation precision of 1st natural periods corresponding to seismic intensity

Preparation and examination of judgment criteria on building damage

Fig.9 shows the relations between the calculated first natural periods and I_{JMA} as the straight lines which in the X (longitudinal) direction and Y (transverse) direction respectively. Each straight line was the approximate one obtained by the least square method with the first natural periods and I_{JMA}, which was added as the seismometers recorded the latest data with seismic intensity 3 or greater. These straight lines were classified into solid lines which showed the maximums and the minimums, and dotted lines which were others between them. In this figure, there are marks of a triangle and a circle which were the values by substituting I_{JMA} of the latest earthquake in 22 November, 2019 for the approximate function calculated with earthquakes before that. According to this figure, we could say that the latest earthquake existed under the maximum first natural period calculated before because these marks are between the solid lines.

Fig.10 shows the calculation accuracy of the first natural periods obtained by using the approximation function of the first natural periods obtained from the relationship between the measured seismic intensity experienced in the past and the first natural periods. The maximum values of ratio, which were obtained by dividing the measured values of the first natural periods by the calculated values, were 1.05 in the X (longitudinal) direction, and 1.13 in the Y (transverse) direction. These maximum values were given in the X (longitudinal) in the 20 July, 2016 earthquake and in Y (transverse) direction in the 5 February, 2016 earthquake respectively. Both of the earthquakes were different from the earthquake which gave the maximum value of the measured seismic intensity, the first natural periods of the building were relatively long without the scale of the measured seismic intensity. On the other hand, it is judged from Fig.5 that no major damage occurred since the primary natural periods do not tend to increase particularly after this earthquake. These ratios can be used as criteria for future damage to buildings. Since the ratios in the case of the most recent earthquake are 1.03 in the X (longitudinal) directions and 1.02 in the Y (transverse) direction, which are lower than the maximum value of the ratio obtained before that, it is clear that no serious damage occurred.

Results and Discussion

Based on observation results so far, we suggested adequate judgement criteria for seismic reinforcement of SRC buildings and examination of damage based on the judgement criteria created. Further earthquake response of the target building will be examined, taking into consideration aging changes, influences of apparent torsion and others in directions.

Acknowledgement

We will pay our respects and deep appreciations to the Kawamoto Ind. Corp. for their corporation to this publication by providing us with seismograph system and others.

Reference:

[1] Aya Kajiwara, Toshinari Ota and Hiroshi Watanabe (2018)" Preparation of Criteria for Damage on Re-reinforced Steel Reinforced Concrete Building Based on Seismic Observation"12th International Workshop on Seismic Microzoning and Risk Reduction, Yokohama, Japan.

[2] Toshinari Ota and Hiroshi Watanabe (2016) "Dynamic Characteristics of a Re-reinforced Steel Reinforced Concrete Building Based on Seismic Observation", Proceedings of the 11th International Workshop on Seismic Microzoning and Risk Reduction, Granada, Spain, 79-86

[3] Toshinari Ota and Hiroshi Watanabe (2017) "Dynamic Characteristics of a Re-reinforced Steel Reinforced Concrete Building Based on Seismic Observation, --Using observed first natural period and predominant period--", The 17th international forum "New Ideas of a New Century, Proceedings of the 17th International Scientific Conference, 3, Khabarovsk, Russia, 323-328

[4] Toshinari Ota (2018) "Proposal of a Method for Damage Detection by Using Dynamic Characteristics of a Re-reinforced Steel Reinforced Concrete Building Based on Seismic Observation", Master's thesis, Kanto Gakuin University (in Japanese).

[5] Koichi Kusunoki (2006) "Residual Seismic Capacity Evaluation of Existing Buildings after an Earthquake", Concrete journal, 44, 5, 102-105 (in Japanese)

[6] Japan Meteorological Agency (15 January, 2020) http://www.jma.go.jp/jma/index.html

[7] Geospatial Information Authority of Japan (15 January, 2020) https://www.gsi.go.jp/

